

# Investigating the True Resolution and Three-dimensional Capabilities of Ground-penetrating Radar Data in Archaeological Surveys: Measurements in a Sand Box

JÜRIG LECKEBUSCH<sup>1,2\*</sup> AND RONALD PEIKERT<sup>3</sup>

<sup>1</sup>*Kantonsarchaeologie, Walchestr. 15, CH-8090 Zurich, Switzerland*

<sup>2</sup>*Department of Prehistory, University of Zurich, Karl Schmid Str. 4, CH-8006 Zurich, Switzerland*

<sup>3</sup>*Institute of Scientific Computing, Swiss Federal Institute of Technology, ETH-Zentrum, CH-8092 Zurich, Switzerland*

**ABSTRACT** The capabilities of ground-penetrating radar (GPR) were studied in a sand box under controlled conditions. To reduce the size of the necessary sand box, the structures were scaled by 50 per cent and the antenna frequency used was doubled from 500 MHz to 900 MHz. Blocks of concrete were buried to model Roman walls. Initial tests showed a great effect of the antenna orientation on the visibility of the structures, which is difficult to account for during a survey. The GPR profiles also showed a significant reduction of the signal amplitude by a strong reflector, obscuring any underlying object.

After three-dimensional migration a single block was perfectly imaged. The signals from a second block, buried below the first, were obscured by several multiples, which prevent its exact detection. This was confirmed by numerical modelling. Comparing real data with modelling results showed that exploding reflector and plane wave models use an incorrect ray path. Only a so-called 1-to-1 adoption model gives comparable results. The measurements with two buried stones are in good agreement with the data from normal surveys. Tests have shown that the superposition of the reflection patterns from single stones makes the detection of any interior structure of a wall impossible. To visualize the three-dimensional information in the data set, a new technique was used: an isosurface of the reflection strength or amplitude envelope was calculated. This procedure makes the full three-dimensional information understandable and reduces the amount of data significantly. The isosurfaces can now be exported and combined with any other archaeological information in a geographical information system (GIS). The speed of this process makes it suitable for large surveys. Copyright © 2001 John Wiley & Sons, Ltd.

*Key words:* ground-penetrating radar; migration; resolution; accuracy; multiple; wavelength; antenna pattern; attenuation; modelling; isosurface; three-dimensional display

---

## Introduction

Ground-penetrating radar (GPR) has become a standard application in archaeological prospection during recent years. Although it is widely

established, there are still several questions that need to be investigated. For example, with regard to the full three-dimensional capabilities of the method, the precision with which archaeological structures are imaged is still to be evaluated. Until now it is unclear whether the interior structure of a wall or two overlying walls on a complex site can be resolved with GPR. To answer these questions, measurements in a sand box were undertaken.

---

\*Correspondence to: J. Leckebusch, Kantonsarchaeologie, Walchestr. 15, CH-8090 Zurich, Switzerland. E-mail: juerg.leckebusch@bd.zh.ch

The controlled conditions also provide excellent data sets for verifying modelling algorithms.

Apart from these questions, the imaging and visualization of the data, especially of large survey areas, is a problem. It is very difficult and time-consuming to understand, extract and interpret the full information content in the processed GPR data. A disadvantage of the manual treatment of the data is that it is subjective. The paper shows a new technique to avoid this.

As an alternative to the sand box, tests in a water tank were considered, because the handling is much easier. Unfortunately, those conditions are very different from real measurements on soil, with different coupling of the antennae to the ground. To have the most similar conditions, we decided to do the experiments in a sand box. To achieve a central area that is undisturbed by any unwanted reflections from the edges of the box it is necessary to construct a sufficiently large sand box. A related box in 1:1 scale would be very large and difficult to build. To overcome these problems, the whole experiment was scaled by 50 per cent. Every measured object had to be scaled by 50 per cent and the antenna frequency was increased from 500 MHz to 900 MHz. A box ( $3.5 \times 2.2$  m wide and 1.55 m high) was built and filled with dried sand (Figure 1).

During the experiment, several tests were made with different archaeological structures in mind. The controlled conditions also allowed checking of several characteristics of the GPR method, especially the antenna pattern and the

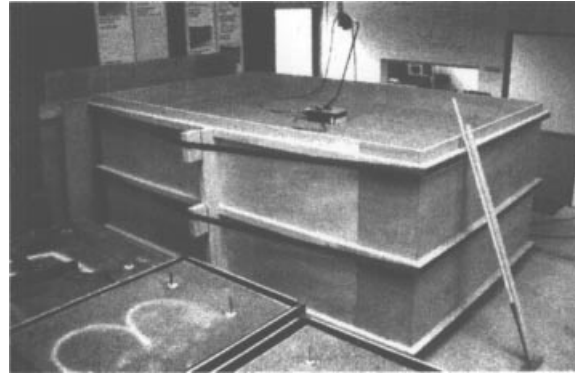


Figure 1. View of sand box with 900 MHz antenna.

reduction of the signal amplitude and penetration depth.

### Set-up

During the time of the experiment, a reference position on the sand box was measured every day. A comparison of these traces shows minimal amplitude variations and only minor changes in the delay time. These results proved that the conditions of the equipment were generally stable and that the small changes can be compensated during data processing.

First, the sand box was filled with sand only (without any structures) in order to obtain an estimate of the background signal and the inhomogeneity of the sand (Figure 2). Reflections from the vertical walls of the box (dipping reflections at the edges) as well as from the bottom

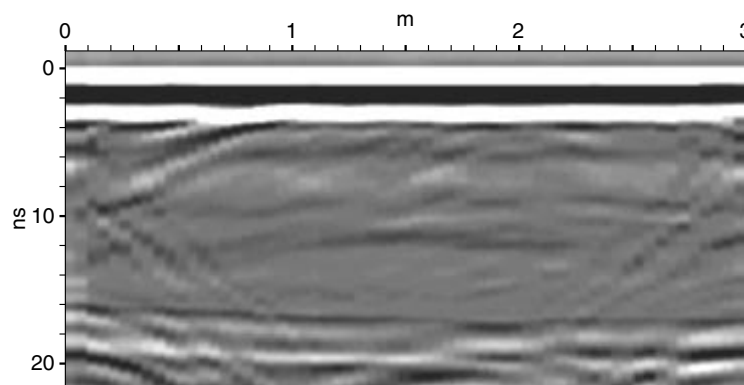


Figure 2. Unmigrated profile through sand box without emplaced objects. Reflections from the side and bottom of the box are clearly visible. A fine layer in the sand appears at about 11 ns in the middle of profile.

(horizontal events at 16–20 ms) are clearly visible. Some other dipping reflections in the left part of the profile (e.g. dipping from 4.0 ns at 1 m to 7.5 ns at 0.5 m) are also visible inside the sand filling, showing the high sensitivity of the GPR method. We assume that these reflections are generated by compaction differences or changes in granularity of the sand. To reduce all these unwanted reflections, this data set was subtracted from every other set before any further processing. The reduction of unwanted signals proved to be not entirely efficient because of some small, inevitable positioning errors in all three directions ( $x$ ,  $y$  and  $z$ ), but nevertheless was able to significantly reduce the noise level (see Figure 3a).

Three surveys of the sand box were carried out (Table 1), each with different buried structures: (i) one wall, (ii) two walls, one above the other with a gap of 10 cm, and (iii) two round stones, one directly on top of the other. Each of these set-ups was used as a model for different situations in archaeological prospection: to model an ancient Roman wall in the sand box we used a block of concrete (22 × 15 cm in cross-section, 95 cm long).

Every data set was processed with exactly the same parameters (Table 2). An important step was the three-dimensional migration to achieve the best results regarding the geometry (Leckebusch, in press). Constant velocity migration tests resulted in a value of  $0.1525 \text{ m ns}^{-1}$ , equivalent to a relative dielectric constant of  $\epsilon_r = 3.9$ , which is very reasonable for sand (Ulriksen, 1982). Time-domain reflectometry (TDR) measurements gave unreasonably high values of  $0.2425 \text{ m ns}^{-1}$ ,  $\epsilon_r = 1.53$ . The very dry condition of the sand made TDR measurements almost impossible and these values were not used further. Small samples

Table 1. Survey set-up and parameters

Sand box dimensions	3.55 × 2.20 × 1.50 m
Effective measuring area	3.00 × 1.70 × 1.25 m
Ground-penetrating radar system	GSSI SIR-10A
Antenna frequency	900 MHz
Recording parameters:	
constant gain	10 dB
stacking	64 traces
filter	none
Spacing:	
inline	0.025 m
crossline	0.050 m

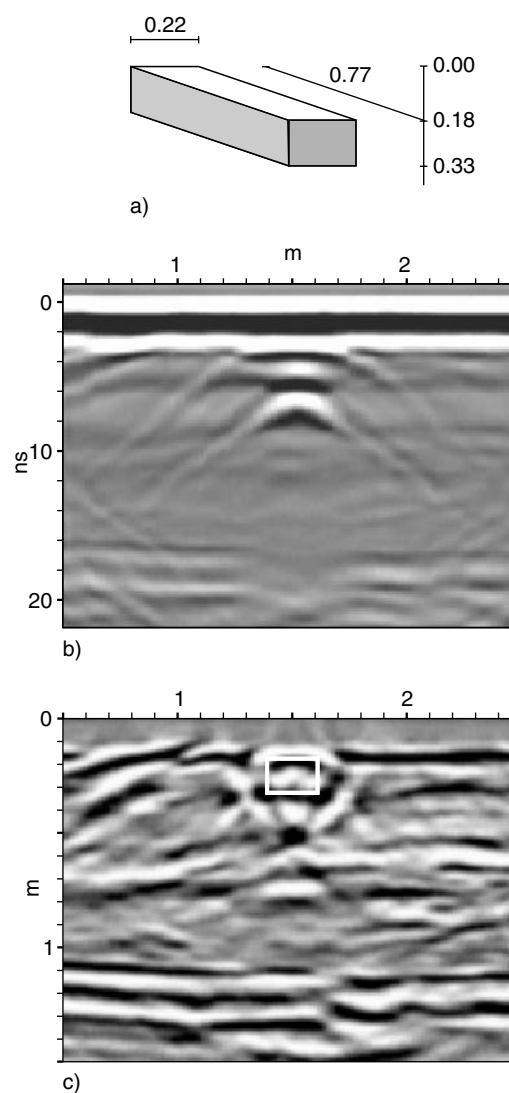


Figure 3. (a) Sand box with one buried block of concrete positioned at 1.5 m; (b) unmigrated and (c) migrated data. White rectangle shows actual position of block. Notice how well the structure is imaged by GPR.

of the concrete were measured with a network analyser and gave velocities of  $0.1142 \pm 0.0073 \text{ m ns}^{-1}$  ( $\epsilon' = 6.9 \pm 0.8$ ,  $\epsilon'' = 0.48 \pm 0.19$ , the real and imaginary part of the relative dielectric constant). The velocity contrast between the sand (background) and the structures searched for is high enough to generate sufficient reflection amplitudes. To define a perfect velocity model of the subsurface the exact geometries and velocities of each searched archaeological structure searched for should be known *a priori*. As this is

Table 2. Processing steps for all normal tests

Noise removal
First arrival alignment
Empty data-set subtraction
Bandpass filter: Butterworth 50–100 1500–2000 MHz
AGC window 6 ns
Stolt three-dimensional migration
Time to depth conversion
Reflection strength
Depth-slice

impossible, a generalization of the velocity model from the surrounding material must be used. This will result in some errors of the migration. Unfortunately the migration equalizes amplitude and therefore enhances fine reflections, such as the remains of the empty data set removal. This makes the final profiles look like this processing step was not very efficient.

### Three-dimensional test: one buried wall

For the first three-dimensional experiment, one block of concrete was buried at a depth of 17.5 cm that corresponds to a depth directly under the ploughing layer in reality. The data processed show excellent mapping, not only in vertical planes but also in horizontal planes (Figure 3). The upper surface of the concrete block is visible as a continuous reflection between 1.4 and 1.6 m and at the correct depth. The lower boundary is also almost continuous but shows a clear focusing of the energy in the corners. This difference between upper and lower boundary might be a result of the fact that the height of the block is approximately one dominant wavelength. The radius of the footprint of the antenna (Annan, 1992)

$$A = \frac{\lambda}{4} + \frac{z}{\sqrt{\epsilon_r - 1}}, B = \frac{A}{2}$$

with a wavelength  $\lambda$  of 20 cm and a depth  $z$  of 17.5 cm is 30 for  $A$  and 15 cm for  $B$  and has the same dimensions as the width of the block. There are no signals from the vertical sides of the block as is expected from theory. After migration the dipping sand layer becomes even more visible (compare with Figure 2). The depth varies from 70 to 60 cm on the left to 30 to 40 cm

on the right. Because the sand box was filled with dried, homogeneous sand, there must be fine differences in grain size or compaction giving a measurable reflection in the data. Two continuous reflections at about 16 and 19 ns are visible across the whole length of the profile. These reflections are generated from the bottom of the sand box (wooden plate), a small air gap and finally the concrete floor of the modern building in which the sand box is located. The reflection beneath this event at position 1.8 m and at 1.2 m depth comes from a metal channel on the concrete floor.

### Three-dimensional test: two buried walls

In archaeological applications it might happen that two structures are on top of each other and only separated by a small gap. To evaluate the limitations of this problem we placed two blocks of concrete directly above each other with a separation of 10 cm (Figure 4). The blocks used were of the same dimensions as in the first experiment.

Looking at the data, we see that the upper block is imaged the same way as in the example with one block. The image of the lower block looks very different. With some imagination, it is possible to see the upper boundary, but all other reflections are smeared out. Nevertheless the depth-slice shows a good horizontal agreement with the real positions. The reduction in vertical resolution can be explained by the small separation of the two blocks of 10 cm, less than one dominant wavelength. It will be shown later, that the image of the lower block is in fact obscured by multiples.

A semi-circular reflection pattern is visible on the depth-slice, surrounding the reflections from the blocks (Figure 4c). On the photograph (Figure 5) taken during the burying of the lower block of concrete, a clear change in grain size on the slope of the ditch can be seen at this position. This gravitational separation of grain sizes is therefore imaged by GPR.

### Three-dimensional test: two stones

Comparing the reflection pattern from a block of concrete (Figure 3b) with data from walls

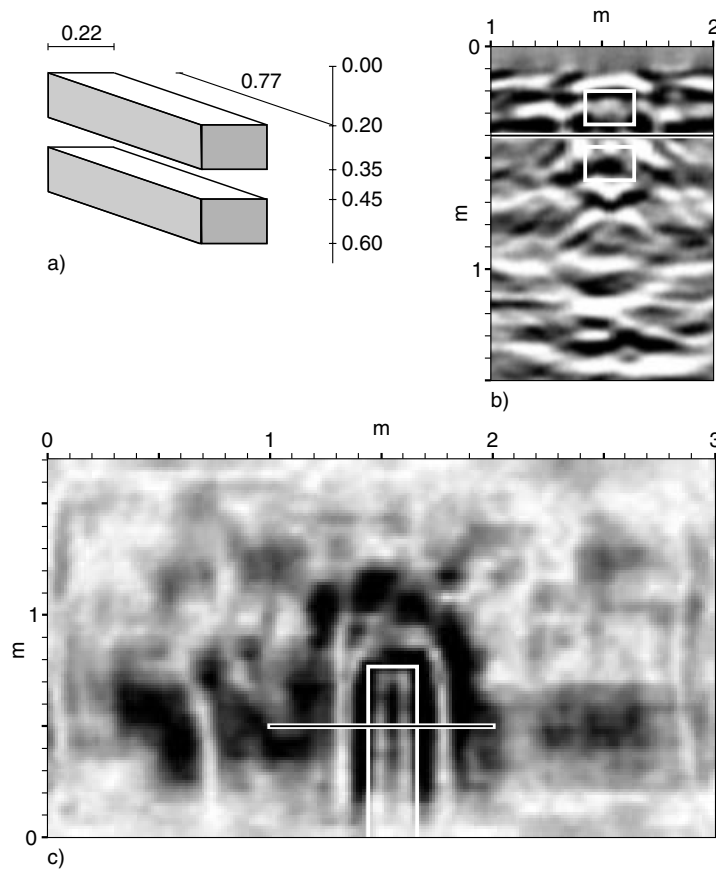


Figure 4. Experiment with two walls. (a) Sketch of the situation, (b) corresponding portion of migrated profile and (c) depth-slice of the reflection strength from 40 to 44 cm. Black lines show position of depth-slice and profile respectively. Positions of blocks are shown in white.



Figure 5. Photograph of sand box during the process of burying the lower wall. Change in grain size at the walls of the ditch due to gravitational separation around the block is clearly visible and could be imaged with GPR (see Figure 4b).

in a realistic situation (Figure 6) shows a clear difference: the concrete shows no reflections from

the interior because the material is homogeneous for the radar waves, whereas in reality we have a pattern of reflections due to the different stones and mortar used. To investigate how the geometry of a wall with many reflections from the interior is mapped, two stones directly on top of one another are buried (Figure 7). This set-up also should allow testing of whether it is possible to resolve the interior structure or not. In previous measurements, we have already resolved images of single stones from a wall (Leckebusch, in press).

The data of this test show a pattern of reflections that looks similar to field data. It clearly can be seen that it is not possible to distinguish the two different stones. Notice also, that the image of the objects is a few centimetres larger than in reality. This is true for all data sets (Figures 3, 4 and 7).

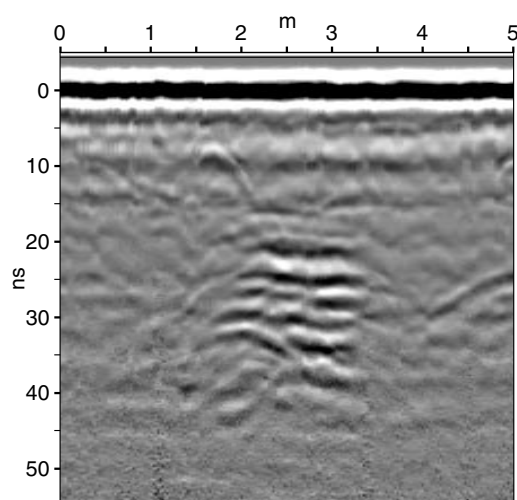


Figure 6. Profile showing typical reflection pattern of a wall as encountered during a survey on a roman town. The survey crosses the wall at a right angle.

### Two-dimensional test: effect of antenna orientation on visibility of structures

The controlled conditions in the sand box allowed performance of a simple test relevant for archaeological prospecting in practice. In routine archaeological surveying, where money and therefore time is a limiting factor, the site is recorded with one orientation of transmitter and receiver antenna only. Radiation or sensitivity patterns of the antennae are not symmetric and therefore interfere with the orientation to the target. This could affect the detectability of the subsurface structures: normally it is assumed that the antenna pattern does not affect the result.

To quantify this, one block of concrete was buried in the sand box and recordings were done on a profile perpendicular across the centre of the block (so that we can assume a two-dimensional case). This profile was measured with 10 different orientations of the antenna in the range of  $0^\circ$  to  $90^\circ$  relative to the profile. The standard orientation of perpendicular-broadside is taken as  $0^\circ$  and parallel-broadside as  $90^\circ$ . The relative orientation and offset of transmitter and receiver was fixed during the tests. In this case, it was only possible to use two-dimensional migration. The necessary velocity, again determined by constant

velocity migration tests, was  $0.1625 \text{ m ns}^{-1}$ . This value is approximately 7 per cent higher than for three-dimensional migration.

The profiles show two different phenomena (Figure 8, see also Figure 3c): passing from  $50^\circ$  to  $60^\circ$ , the concrete block becomes almost invisible in the data. This is an effect of the radiation pattern of the antenna (Annan and Cosway, 1992; Lehmann *et al*, in press). Because more energy is radiated parallel to the antenna, a perpendicular-broadside configuration receives more energy from a reflector in total (along the hyperbola) than a parallel-broadside set-up. Furthermore, there is a different coupling of the signal to the ground, as can be seen in the first reflection. The antenna is designed to be used in perpendicular-broadside orientation, which is facilitated by some sliding plates underneath. Pulling the antenna with another orientation will result in a higher mechanical resistance and therefore fill up the air gap between antenna and sand. This has the same effect as changing the height of the antenna above ground and significantly changes the coupling (Annan *et al*, 1975; Annan, 1992). Nevertheless the experiment shows a clear dependence of the detectability of a structure on the relative orientation of the antenna to the structure. This effect normally is ignored in archaeology, and is very difficult to take into account because the orientation of the structures may vary and even be unknown.

### Reduction of the signal amplitude and penetration depth

The situation where different structures are overlying each other is encountered very often in archaeology. The question is, whether overlying objects or interfaces affect the reflections from the lower structures. This can be seen best in the data from the experiment with one buried block of concrete (Figure 9 and compare Figures 2 and 3b). It is clearly visible that the overlying block masks the reflections from the bottom of the sand box. The signal delay from the lower velocity in the wall is within a few nanoseconds and therefore makes it almost negligible. The signal reduction can be explained by the high amount of energy that is already reflected back

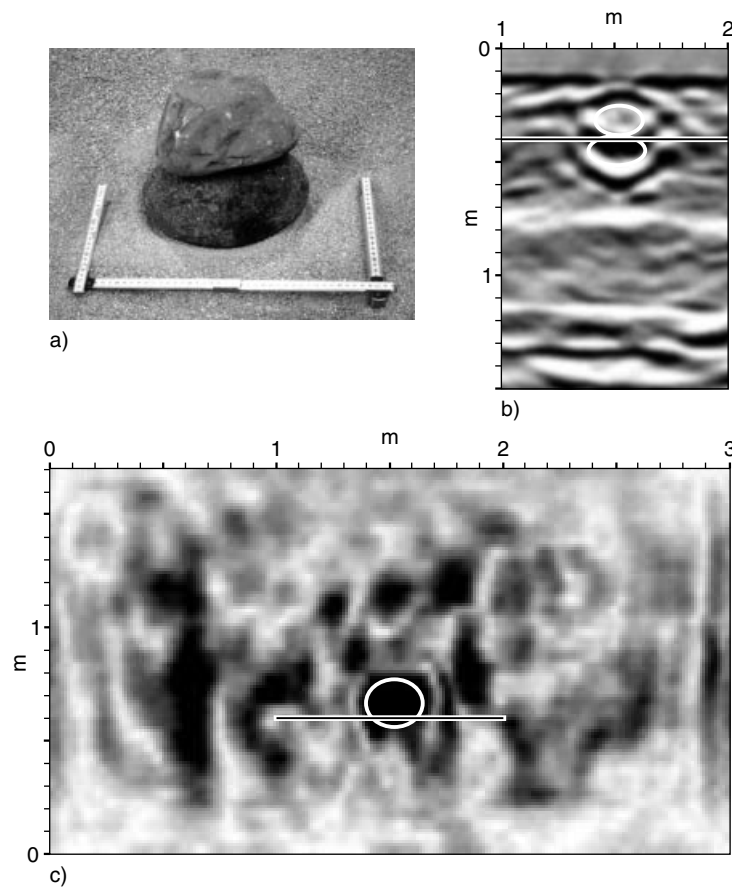


Figure 7. Experiment with two stones. (a) Photograph of the two stones before sand was poured over them. Ground-penetrating radar data allow for excellent imaging (b) in the migrated profile and (c) the depth-slice of the reflection strength from 40 to 44 cm. Black lines show position of depth-slice and profile respectively. Positions of stones are indicated in white.

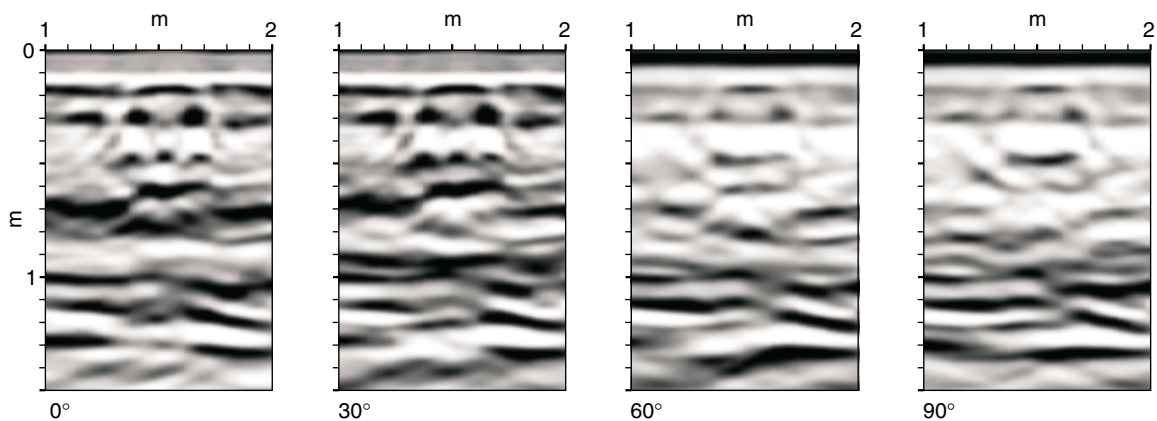


Figure 8. Effect of change in antenna orientation along same profile. Data are two-dimensionally migrated. Notice how difficult it is to define the position of the single wall in profiles with an antenna orientation closer to parallel-broadside than to perpendicular-broadside. Geometry is shown in Figure 3a.

from the concrete to the surface: only reduced energy reaches the bottom. Using the measured relative dielectric constants of the materials an estimate of the reflection coefficient from the first block can be calculated (Reynolds, 1997)

$$R = \frac{\sqrt{\epsilon_1} - \sqrt{\epsilon_2}}{\sqrt{\epsilon_1} + \sqrt{\epsilon_2}}, = 0.14,$$

where  $\epsilon_1$  and  $\epsilon_2$  are the relative dielectric constants of the sand and the concrete, respectively, and  $R$  is the reflection coefficient. The energy therefore is reduced twice by 17 dB from the upper and from the lower interface of the upper wall. Without taking spherical spreading and attenuation into account, this is already about one-third of the dynamic range of a GPR system with 100 dB. Therefore, it is difficult to record any significant signal from the bottom of the sand box, where there is a strong reflecting object above. This is a very important effect that should be taken into account for every survey, not only in archaeology.

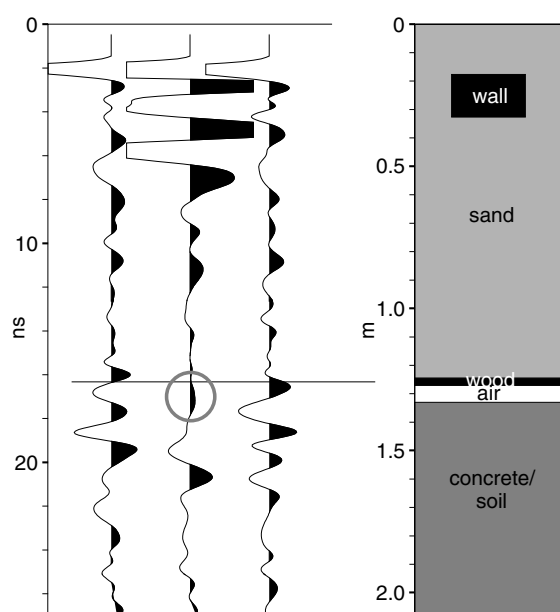


Figure 9. Reduction of signal amplitudes under reflecting structure. Although the traces to each side of the block show clear reflections from the bottom of the sand box, the amplitudes disappear in background noise under block (middle trace), marked with a circle. Lower velocity of wall caused a small delay of the event. The same effects are visible by comparing Figures 2 and 3a. Strong reflection in middle trace at 20 ns is from an interface in the concrete.

## Modelling

Detailed measurements under controlled conditions are an excellent reference for the testing of numerical forward algorithms. Full waveform algorithms such as finite-difference or pseudo-spectral methods allow the complete wavefield to be modelled, including attenuation and dispersion effects, which makes them advantageous over ray methods (Goodman, 1994). Finite-difference experiments with two buried blocks of concrete were achieved for these computations. The result of the modelling was considered in exactly the same way as the original field data, excluding the first three steps, which were not necessary with synthetic data (cf. Table 2). Therefore, the migrated synthetic and real data are directly comparable to each other. Plane wave (Carcione, 1996; Xu and McMechan, 1997; Bergmann *et al*, 1998) or exploding reflector methods (Zeng *et al*, 1995; Bergmann and Holliger, in press) are standard in electromagnetic forward modelling to acquire a GPR survey. However, these approaches show completely undermigrated profiles (Figure 10b and c): this is the result of an incorrect ray path assumption for the calculation and the inability to model correctly phases and travel times of multiple reflections. Only placement of a single source at the surface and calculating the complete wavefield for each trace location yielded comparable results (Bergmann and Holliger, in press), called 1-to-1 adaption (Figure 10d). Only the frequency content and the wave velocity seem to be somewhat higher than in reality. There are still some overmigrated reflection events, which are obvious indications of multiple waves. These multiples at a depth of 50 and 55 cm in fact obscure the image of the lower block of concrete both in synthetic data and in the sand box measurements (see Figure 4).

## Extraction of three-dimensional information

Ground-penetrating radar is capable of giving a three-dimensional image of the subsurface if the area is surveyed on a sufficiently dense grid. However, this full three-dimensional capability

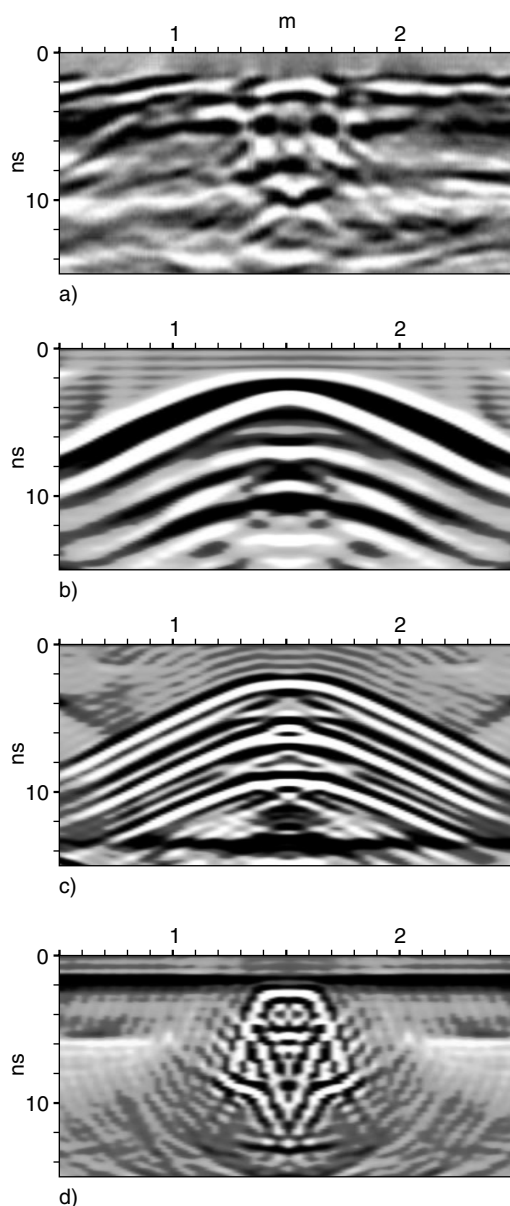


Figure 10. Comparison of data from experiment and different modelling algorithms. Time-migrated profiles over two buried walls (for geometry see Figure 4a). (a) Real data, (b) plane wave, (c) exploding reflector and (d) 1 to 1 adaption.

is rarely used for imaging structures directly. The conventional way to display the information in the GPR data is by profiles and horizontal time- or depth-slices. Nevertheless, these are only two-dimensional representations (Figure 11), which are very difficult to understand for non-specialists. The next step to improve

the visualization of the data is more or less automatic picking of layers and subsequent three-dimensional display with shaded relief of the picked interfaces (Leckebusch, 1998; Leckebusch, 2000). Unfortunately, this procedure is very time-consuming. These problems can be overcome by calculating isosurfaces of the whole data set (Figure 12). This interpretation technique is much less subjective and also very fast and robust. Another important point is that this procedure significantly reduces the amount of data. To calculate an isosurface the grid data are converted to the reflection strength or amplitude envelope by a Hilbert transformation, which then is scanned for a user supplied level. In the case of a normal wall consisting of individual stones, the isosurface should image the envelope of the object searched for. Without the calculation of the reflection strength the resulting isosurface will be split into individual parts because of the amplitudes of positive and negative traces. The quality of the result can be further improved by accepting only objects with volumes inside a specified range. The largest volume usually is the surface reflection, whereas small extracted objects can be regarded as unwanted noise or objects with no archaeological relevance. Each object can now be colour-coded or exported to a geographical information system (GIS). In the latter, each structure can be described together with other archaeological evidence. The data processing speed makes this procedure suitable for large surveys. There is only one major problem: if the reflection strength varies significantly for a single buried object or structure, it might be separated during the calculation of the isosurface or it might have a hole in it. This can be clearly seen for the reflections from the bottom of the sand box and for the sand layer (Figure 12). In general, the calculation of the isosurfaces extracts the important features and makes the complete geometry available for archaeologists in an easily understandable way.

## Conclusions

Measurements in a sand box have shown the good imaging capabilities of GPR in all three dimensions, shown for the case of a model of a typical Roman wall. For a detailed analysis

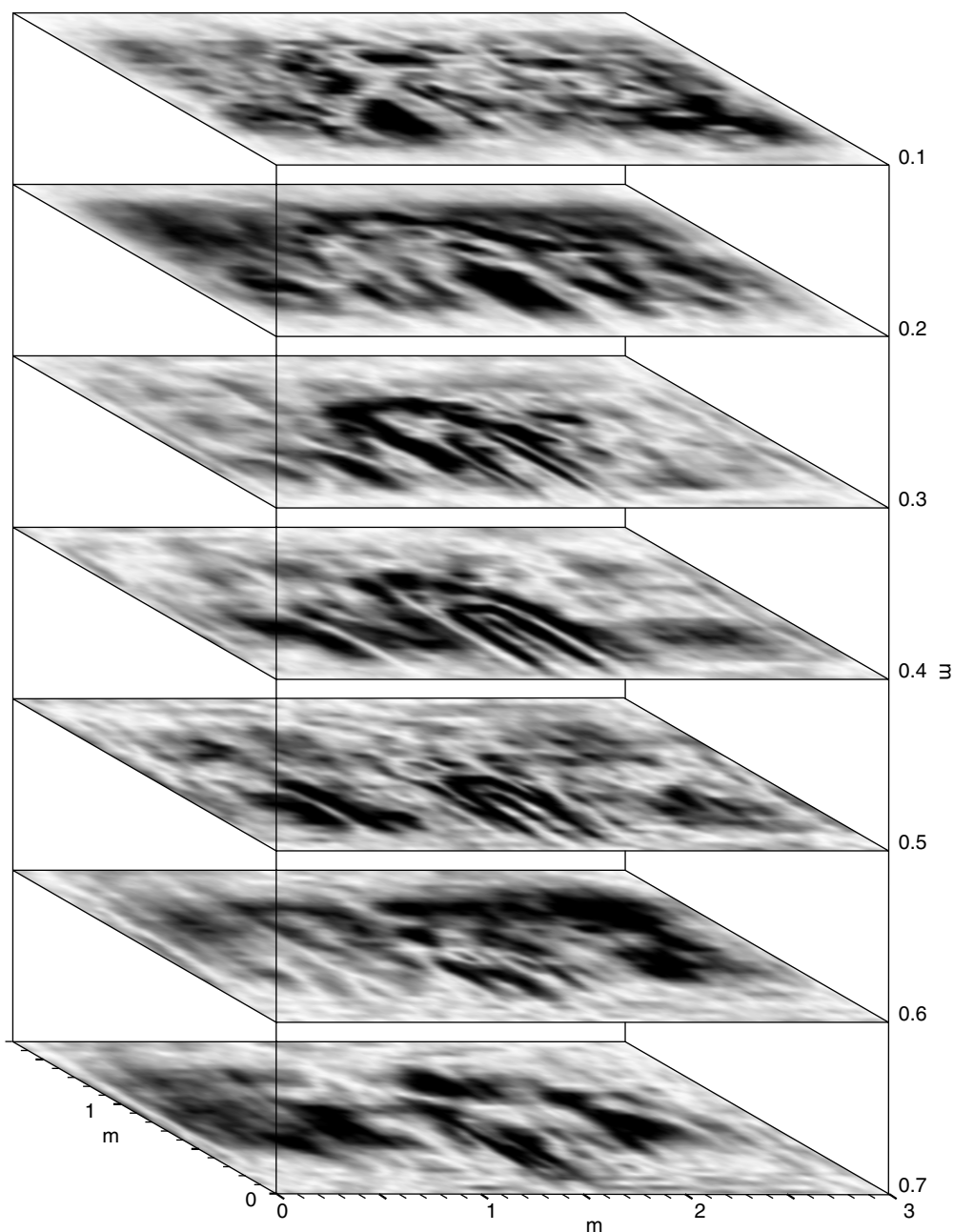


Figure 11. Stack of several depth-slices through the data cube with two buried walls. The reflection strength is integrated over a depth range of 4.5 cm starting at the levels indicated.

of the data it is important to note that the structures appear a little larger than they are in reality. If the structures are too close together, the image of the lower one is disturbed by multiple reflections, which is confirmed by modelling. The data set taken over two buried stones shows

that it is impossible with the antenna frequency used to resolve single stones in the interior of a wall. The controlled conditions allowed imaging the effect of a structure on any other reflector below. Because the energy reaching the lower structure might be too low to be recorded at

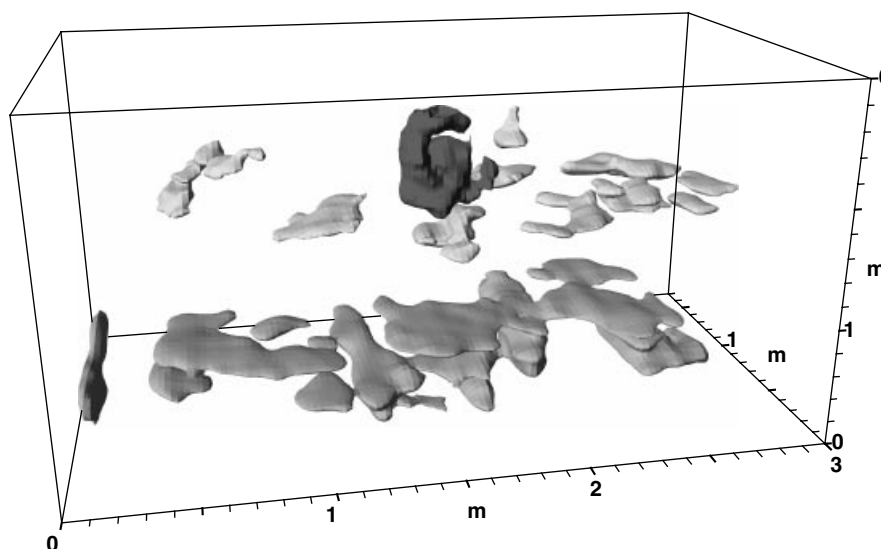


Figure 12. Isosurfaces extracted from the GPR data. Display of the sand box with two buried stones in shaded relief. Signals are colour coded in grey-scale tones. Stones are displayed in dark grey, bottom of sand box and concrete floor in grey and subhorizontal layer in sand in lightest grey.

the surface, a continuous reflection surface might appear interrupted in the GPR data. The effect of the orientation of the antenna with regard to the structure imaged is shown very clearly. Comparison of the real with synthetic data showed that a plane wave or exploding reflector model assumes an incorrect ray path. Only a so-called 1-to-1 adoption model produces a good agreement.

The limitations of visualization and interpretation of the GPR data by using profiles or time- or depth-slices have been overcome by calculating an isosurface with a user defined amplitude level through the whole data set. For the purpose of having only positive amplitudes the reflection strength or trace envelope is determined first. This procedure is very efficient and uses the three-dimensional capabilities of GRP previously unexploited. At the same time it reduces the amount of data and allows a data export to a GIS, for example.

### Acknowledgements

I would like to thank Dr M. Partl and J. Hugen-schmidt especially for rebuilding the sand box with the necessary dimensions and members of the EMPA for their help during the measurements. All modelling was kindly

done by Dr T. Bergmann, formerly of the Institute of Geophysics, Swiss Federal Institute of Technology, Zurich. H. Horstmeyer from the same institute kindly assisted with processing and his advice greatly improved the manuscript.

### REFERENCES

- Annan AP, Cosway SW. 1992. Simplified GPR beam model for survey design. *62nd Annual International Meeting of the Society of Exploration Geophysicist*, New Orleans, 356–359.
- Annan AP, Waller WM, Strangway DW, Rossiter JR, Redman JD, Watts RD. 1975. The electromagnetic response of a low-loss, 2-layer, dielectric earth for horizontal dipole excitation. *Geophysics* **40**: 285–298.
- Annan P. 1992. *Ground Penetrating Radar: Workshop Notes*. Sensors & Software Inc.: Mississauga, Ontario.
- Bergmann T, Holliger K. in press. Full-waveform modelling of zero-offset georadar sections: overview and application. *Journal of Applied Geophysics*.
- Bergmann T, Robertsson JOA, Holliger K. 1998. Finite-difference modelling of ground-penetrating radar data in dispersive and attenuating media. *Geophysics* **63**: 856–867.
- Carcione JM. 1996. Ground-penetrating radar: wave theory and numerical simulation in lossy anisotropic media. *Geophysics* **61**: 1664–1677.
- Goodman D. 1994. Ground-penetrating radar simulation in engineering and archaeology. *Geophysics* **59**: 224–232.

- Leckebusch J. 1998. Automatisierung von Radar- und Widerstandsmessungen in Verbindung mit dreidimensionaler Radardatenverarbeitung. *Materialhefte zur Archäologie in Baden-Württemberg* **41**: 77–80.
- Leckebusch J. 2000. Two- and three-dimensional ground-penetrating radar surveys across a medieval choir: a case study in archaeology. *Archaeological Prospection*. **7**: 189–200.
- Lehmann F, Boerner DE, Holliger K, Green AG. in press. Vectorial nature of georadar data: implications for data acquisition and processing. *Geophysics*.
- Reynolds JM. 1997. *An Introduction to Applied and Environmental Geophysics*. Wiley: Chichester.
- Ulriksen P. 1982. *Application of Impulse Radar to Civil Engineering*. Lund University of Technology, Lund, Sweden.
- Xu T, McMechan GA. 1997. GPR attenuation and its numerical simulation in 2.5 dimensions. *Geophysics* **62**: 403–414.
- Zeng X, McMechan GA, Cai J, Chen HW. 1995. Comparison of ray and Fourier methods for modelling monostatic ground-penetrating radar profiles. *Geophysics* **60**: 1727–1734.